Effects of Oxygen Concentration on the Reaction to Fire of Cross-Laminated Timber in a Controlled-Atmosphere Cone Calorimeter

Véronique Marchetti, Gaelle Fontaine, Adèle Lamandé, Serge Bourbigot

Metadata of the article that will be visualized in OnlineFirst

ArticleTitle	Effects of Oxygen Concentration on the Reaction to Fire of Cross-Laminated Timber in a Controlled-Atmosphere Cone Calorimeter	
Article Sub-Title		
Article CopyRight	Springer Science+Business Media, LLC, part of Springer Nature (This will be the copyright line in the final PDF)	
Journal Name	Fire Technology	
Corresponding Author	FamilyName	**Marchetti**
	Particle	
	Given Name	**Véronique**
	Suffix	
	Division	
	Organization	Centre Scientifique et Technique du Bâtiment (CSTB), University of Paris-Est
	Address	Champs-sur-Marne, France
	Phone	
	Fax	
	Email	veronique.marchetti@cstb.fr
	URL	
	ORCID	
Corresponding Author	FamilyName	**Fontaine**
	Particle	
	Given Name	**Gaëlle**
	Suffix	
	Division	
	Organization	CNRS, INRAE, Centrale Lille, UMR 8207 - UMET - Unité Matériaux et Transformations, University of Lille
	Address	59000, Lille, France
	Phone	
	Fax	
	Email	gaelle.fontaine@centralelille.fr
	URL	
	ORCID	http://orcid.org/0000-0002-7113-1687
Author	FamilyName	**Lamandé**
	Particle	
	Given Name	**Adèle**
	Suffix	
	Division	
	Organization	Centre Scientifique et Technique du Bâtiment (CSTB), University of Paris-Est
	Address	Champs-sur-Marne, France
	Division	
	Organization	CNRS, INRAE, Centrale Lille, UMR 8207 - UMET - Unité Matériaux et Transformations, University of Lille
	Address	59000, Lille, France
	Phone	
	Fax	
	Email	
	URL	
	ORCID	

Author	FamilyName	**Bourbigot**
	Particle	
	Given Name	**Serge**
	Suffix	
	Division	
	Organization	CNRS, INRAE, Centrale Lille, UMR 8207 - UMET - Unité Matériaux et Transformations, University of Lille
	Address	59000, Lille, France
	Division	
	Organization	Institut Universitaire de France (IUF)
	Address	Paris, France
	Phone	
	Fax	
	Email	
	URL	
	ORCID	

Schedule	Received	29 Oct 2022
	Revised	
	Accepted	13 Nov 2023

Abstract	This paper deals with the fire reaction as well as the gas and aerosol production of Cross-Laminated Timber (CLT) submitted to fire in oxygen-depleted environments. A Controlled-Atmosphere Cone Calorimeter (CACC) coupled to a Fourier Transform Infrared (FTIR) spectrometer and an Electrical Low Pressure Impactor (ELPI) was used for this purpose. This combination enabled simultaneous assessments of Mass Loss Rate (MLR), evolved gases (qualitatively and quantitatively) and aerosols (size distribution and concentration) in the smoke. Several oxygen levels (21, 18, 15 and 10% O_2) were studied at an external heat flux of 50 and 20 kW/m2. The combination of these two parameters allowed the response of CLT to be classified according to different fire scenarios. Indeed, an oxygen decrease shifted the combustion towards incompleteness or even prevented combustion. The production of carbon monoxide and methane was significantly promoted as well as acetaldehyde and ethene in some cases. The aerosol size distribution was slightly affected by oxygen depletion. Furthermore, decreasing the heat flux greatly reduced the decomposition rate but also promoted the production of unburnt gases.

Keywords (separated by '-')	Cross-laminated timber - Controlled-atmosphere cone calorimeter - Oxygen vitiation - Gases - Aerosols
Footnote Information	

Journal : 10694_FIRE | Dispatch : 19-12-2023 | Pages : 26
MS NO : 1518 | ☐ LE ☑ CP | ☐ TYPESET ☑ DISK

Fire Technology

https://doi.org/10.1007/s10694-023-01518-0

Effects of Oxygen Concentration on the Reaction to Fire of Cross-Laminated Timber in a Controlled-Atmosphere Cone Calorimeter

Adèle Lamandé, Centre Scientifique et Technique du Bâtiment (CSTB), University of Paris-Est, Champs-sur-Marne, France; CNRS, INRAE, Centrale Lille, UMR 8207 - UMET - Unité Matériaux et Transformations, University of Lille, 59000 Lille, France

Véronique Marchetti, Centre Scientifique et Technique du Bâtiment (CSTB), University of Paris-Est, Champs-sur-Marne, France*

Serge Bourbigot, CNRS, INRAE, Centrale Lille, UMR 8207 - UMET - Unité Matériaux et Transformations, University of Lille, 59000 Lille, France; Institut Universitaire de France (IUF), Paris, France

Gaëlle Fontaine, CNRS, INRAE, Centrale Lille, UMR 8207 - UMET - Unité Matériaux et Transformations, University of Lille, 59000 Lille, France*

Received: 29 October 2022/**Accepted:** 13 November 2023

Abstract. This paper deals with the fire reaction as well as the gas and aerosol production of Cross-Laminated Timber (CLT) submitted to fire in oxygen-depleted environments. A Controlled-Atmosphere Cone Calorimeter (CACC) coupled to a Fourier Transform Infrared (FTIR) spectrometer and an Electrical Low Pressure Impactor (ELPI) was used for this purpose. This combination enabled simultaneous assessments of Mass Loss Rate (MLR), evolved gases (qualitatively and quantitatively) and aerosols (size distribution and concentration) in the smoke. Several oxygen levels (21, 18, 15 and 10% O_2) were studied at an external heat flux of 50 and 20 kW/m^2. The combination of these two parameters allowed the response of CLT to be classified according to different fire scenarios. Indeed, an oxygen decrease shifted the combustion towards incompleteness or even prevented combustion. The production of carbon monoxide and methane was significantly promoted as well as acetaldehyde and ethene in some cases. The aerosol size distribution was slightly affected by oxygen depletion. Furthermore, decreasing the heat flux greatly reduced the decomposition rate but also promoted the production of unburnt gases.

Keywords: Cross-laminated timber, Controlled-atmosphere cone calorimeter, Oxygen vitiation, Gases, Aerosols

* Correspondence should be addressed to: Véronique Marchetti, E-mail: veronique.marchetti@cstb.fr; Gaëlle Fontaine, E-mail: gaelle.fontaine@centralelille.fr

Journal : 10694_FIRE | Dispatch : 19-12-2023 | Pages : 26
MS NO : 1518 | LE | CP | TYPESET | DISK

1. Introduction

In recent years, there has been a great deal of interest in sustainable construction, with the objective of developing energy-efficient buildings with a low carbon footprint. To fulfill this objective, renewable and/or recycled construction materials are increasingly used, as wood-based materials. In the building field, Cross-Laminated Timber (CLT) is widely used because of its structural properties. With low weight and fast construction times, CLT challenges the use of traditional dense materials like steel and concrete. However, like most organic-based materials, CLT decomposes when exposed to fire. Thus, it is important to study its behavior under different fire scenarios to implement suitable protection methods to ensure the safety of people. Especially, knowledge of gas and aerosol emissions from the thermal decomposition of CLT is paramount. Indeed, during a building fire, most deaths are due to smoke release [1]. Smoke reduces visibility, causes impaired vision and respiratory problems due to irritating and asphyxiating gases. Consequently, this leads to impairment of escape and increases the time to escape and the probability of injuries or death [2]. To ensure safe evacuation, the standard ISO 13571 [3] subdivides the risks to people escaping a fire into the effects of heat, asphyxiant and irritant gases and visual obscuration by smoke. Each component is assessed separately and untenability is defined when one of the components reaches a level that prevents escape. This underlines the need to assess the toxicity of materials to have a better understanding of phenomena occurring during a fire and to improve fire safety engineering. Toxicants production and yield depend on the material composition and the fire conditions including oxygen concentration and temperature. An under-ventilated or low oxygen level (vitiated) atmosphere increases the production of dangerous gases for humans. Indeed, the oxygen level quickly decreases until it no longer allows complete combustion. A dense, carbon monoxide (CO) rich smoke as well as other toxic gases and non-toxic gases are produced. A complete assessment of the thermal decomposition of materials with gaseous emissions and aerosols production is crucial for fire safety.

To date, there are many bench-scale devices available but there is no international agreement or standard on how to assess this toxicity. The main challenges are to correlate results with real scale as well as to simulate and control different fire scenarios. The Controlled-Atmosphere Cone Calorimeter (CACC) is a modified design from the Cone Calorimeter developed by V. Babrauskas and standardized in ISO 5660–1 [4]. The standard cone calorimeter is widely used to assess the reaction to fire of a material but as its design is open, it represents well-ventilated conditions and it does not enable reduced oxygen atmospheres. Consequently, research focused on the development of enclosed cone calorimeters where the oxygen level of the atmosphere can be controlled. Werrel categorized them into two designs: closed designs and open designs [5]. These latter have no connection between the exhaust hood and the enclosure. Several open designs were set up to study the reaction to fire of various materials, *e.g.* polymethylmethacrylate (PMMA) [5–10], polyethylene (PE) [7, 11], polyisocyanurate (PUR) [12], acrylonitrile butadiene styrene (ABS) [7, 13], polyvinyl chloride (PVC) [10, 14], sandwich

Journal : 10694_FIRE | Dispatch : 19-12-2023 | Pages : 26
MS NO : 1518 | LE | CP | TYPESET | DISK

material [15] or wood [16]. As there was no international agreement on the CACC design nor the experimental protocol, Marquis et al. [6] investigated the interpretation and accuracy of results with different setup. They observed that the design of the combustion enclosure may affect the material burning behavior and the accuracy of measurement. Therefore, they suggested constructing a chimney between the enclosure and the exhaust hood to reduce the post-oxidation phenomenon. From this work, the CACC and the experimental protocol associated are now standardized with ISO 5660–5:2020 [17]. In this standard, new equations developed by Werrel et al. [5] to calculate the Heat Release Rate (HRR) are presented. Indeed, the exhaust gases are diluted by excess air drawn from the laboratory surroundings. The heat-induced changes in the dilution ratio affect the measurement of the oxygen and the calculation of the HRR. The error in the HRR calculation increases at a significant order of magnitude (≈ 30%) when the oxygen content in the enclosure is decreased below 18 vol % [5]. Thus, Werrel et al. [5] considered the variations in the flow rate of the ambient air from the laboratory drawn into the exhaust hood to avoid inaccurate HRR calculations.

Work done on several CACC designs and materials has shown trends in the effect of oxygen. Indeed, the HRR [7, 8] and the Mass Loss Rate (MLR) [7, 8, 18] decrease when oxygen concentration decreases (vitiation). On the contrary, the carbon monoxide production [7, 19] increases with vitiation whereas the time to ignition remain unchanged [8]. However, the effect of oxygen on the fire behavior of CLT in a CACC has never been studied. More specifically, there is a lack of data on the gaseous emissions and the aerosols production of CLT in vitiated environments.

This paper depicts the results of the effects of oxygen concentration on the reaction to fire and gas and aerosol production of CLT in a CACC. To have a better understanding of the complex phenomena occurring, a homemade bench is designed where a Fourier Transform Infrared (FTIR) spectrometer as well as an Electrical Low Pressure Impactor (ELPI) are coupled to the CACC. Particularly, the samplings for FTIR and ELPI analysis are made in the chimney instead of in the exhaust duct in order to limit the loss of species due to dilution/oxidation with ambient air. The experiments are realized at an irradiance of 50 and 20 kW/m^2 to assess the fire risks of CLT under different fire scenarios, respectively well-ventilated fires and smoldering.

2. Material and Method

2.1. Material

The material used in this study is a commercial Cross-Laminated Timber (CLT) made from spruce. The panels used consist of two 20 mm thick plies glued perpendicular to each other. The glue used is polyurethane based and it does not release formaldehyde. The sample dimensions are 100 mm long, 100 mm wide and 40 mm thick. It has a specific gravity of 500 kg/m^3, a thermal conductivity of 0.12 W/m.K and a heat capacity of 1600 J/kg K (Table 1).

Journal : 10694_FIRE | Dispatch : 19-12-2023 | Pages : 26
MS NO : 1518 | ☐ LE ☑ CP | ☐ TYPESET ☑ DISK

Table 1
CLT Properties Given by the Manufacturer

Specific gravity	500 kg/m^3
Thermal conductivity	0.12 W/m K
Heat capacity	1600 J/kg K

The specimens are conditioned at 23 ± 2 ℃ and at a relative humidity of 50 ± 5% until the mass is constant, in order to reach a moisture of wood close to 11% as described in the standard EN 13238 [20].

2.2. *Controlled-Atmosphere Cone Calorimeter*

Very recently an experimental standard was released, it is entitled "ISO 5660–5: Heat release rate (cone calorimeter method) and smoke production rate (dynamic measurement) under reduced oxygen atmospheres" [17]. It specifies how to use the cone calorimeter to perform tests in controlled atmospheres. The device is able to work under 1% to 21% of oxygen and to deliver between 10 and 180 L/min of gas. The enclosure, described in Figure 1, is a stainless-steel box of 37 30 30 cm^3 in dimensions with the standard cone heater on top, a door and a window. Inside, there is a load cell and two gas inlet ports. The atmosphere is adjusted by control of the volume flow rate of air and nitrogen, each with a rotameter and monitored by an additional oxygen analyzer that is linked to the enclosure. Moreover, to avoid excessive heating and radiation of the system, a cooling ring is set between the cone heater and the top of the enclosure as well as a cooling hood on the load cell and a cooling serpentine around the load cell's rod.

The experimental method is similar to that of the standard cone calorimeter. The surface area of the sample is 100 100 mm^2. The sample can be exposed to a constant irradiance level up to 100 kW/m^2. Above the sample, a spark plug ignites the flammable gases that might be released. These gases are then collected in the exhaust hood and send through a duct provided with thermocouples, pressure sensor, smoke measurement and a ring probe for O_2, CO and CO_2 analyzers. As a result, heat release rate, mass loss rate, smoke density and gas concentration are assessed.

A drawback of the CACC is the possible post-oxidation of the fire effluent between the enclosure and the exhaust sampling point that would modify HRR and gas measurements. To overcome this issue, the standard specifies to set a chimney of 60 cm long and of 11.5 cm in diameter above the cone heater. It can be made of metal or of quartz; the differences have been discussed in [6].

In this study, the CACC depicted above is used but with some modifications. Indeed, to avoid heat losses, the four walls of the enclosure are insulated with 25 mm calcium silicate panels. Moreover, a new metallic chimney is set to ensure better sampling of effluents.

Journal : 10694_FIRE | Dispatch : 19-12-2023 | Pages : 26
MS NO : 1518 | ☐ LE ☑ CP | ☐ TYPESET ☑ DISK

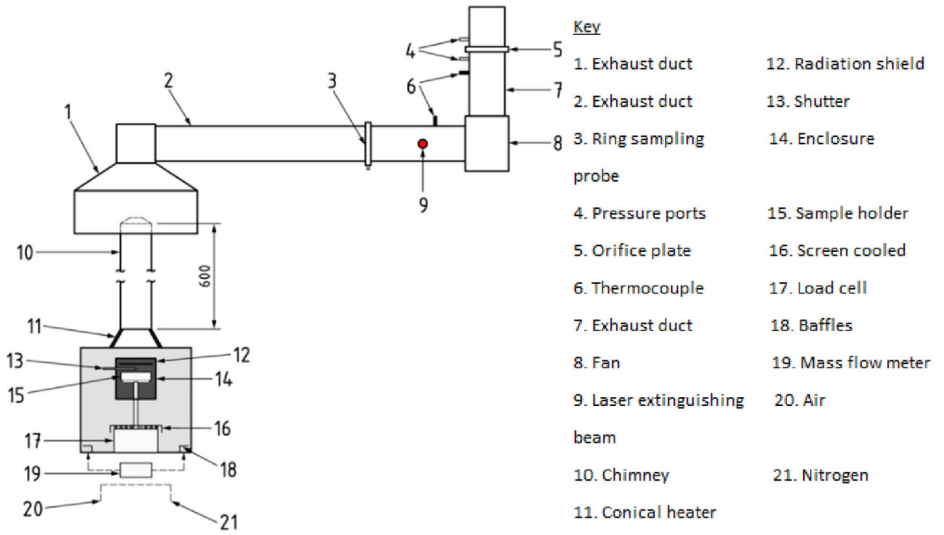

Figure 1. CACC design from ISO 5660–5 [16].

2.3. Controlled-Atmosphere Cone Calorimeter Coupled with FTIR and ELPI

To study the influence of oxygen concentration on the gas production and the aerosol size distribution, two devices were respectively coupled to the CACC: a Fourier Transform Infrared spectrometer and an Electrical Low Pressure Impactor. Instead of classical sampling in the duct, the raw sampling method is used in this study. It was recently developed in order to avoid the loss of effluent when assessing its composition. Indeed, the effluents can condensate while being transported and more importantly when diluted species are lost due to their low concentration (acrolein or formaldehyde for example). Dilution lowers the dew point of the sample so that the water vapor in the effluents does not condense when the sample is cooled by dilution [21]. Consequently, the sampling of the effluent is made in the chimney instead of in the exhaust duct. Further details on the sampling method can be found in literature [10, 12, 21, 22].

In this study, a new metallic chimney (Figure 2a), was designed in order to insert a sampling probe for the FTIR and another one for the ELPI. The chimney is 60 cm long and of 11.5 cm in diameter with its top diameter reduced to 5 cm to assure a sufficient velocity flow of the smoke in the duct. The FTIR sampling probe (Figure 2b) is located near the outlet of the cone and is composed of two flute probes of four holes each to have a homogenous mixture. The holes face away the stream of effluent. The ELPI measurement consists in a single point probe that ensures isokinetic sampling.

An Antaris IGS FTIR spectrometer equipped with a nitrogen Mercury Cadmium Telluride (MCT) detector, 0.2L volume gas cell, and a 2 m optical path length is set. Each scan was taken at 1.76 s and 0.5 cm^{-1} as spectral resolution. At the output of the chimney, the gases are transported through a PTFE line. The

Journal : 10694_FIRE | Dispatch : 19-12-2023 | Pages : 26
MS NO : 1518 | ☐ LE ☑ CP | ☐ TYPESET ☑ DISK

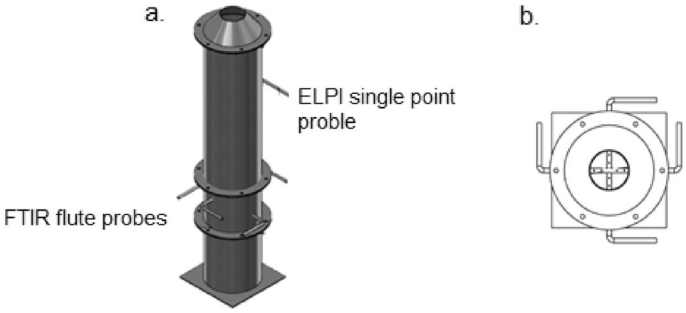

Figure 2. (a) designed metallic chimney for raw sampling; (b) top view of FTIR probes.

FTIR gas cell as well as the PTFE gas transport line are heated at 180 ℃ to avoid condensation. In the end, gases are cooled down, dried, filtered and then evacuated with a membrane pump. The gas cell was kept at a constant pressure of 650 Torr with a pressure gauge with regulating valve. Each gas (CO_2, CO, H_2O, CH_4, CH_2O, C_2H_4O, C_2H_4, C_3H_6) is calibrated using the Classical Least Square (CLS) algorithm. For each gas, a dilution range was analyzed with the FTIR. Characteristic peaks on FTIR spectra were carefully selected by considering all the unavoidable interferences between substances [23].

ELPIs are cascade impactors widely used to measure in real-time the particle size distribution and the concentration of aerosols. An ELPI as well as two diluters from Dekati are set. The ELPI principle consists of three main steps. First, the sampled aerosols are subjected to a unipolar positive ion environment in a corona charger where they are electrically charged. Then, the charged particles enter a low-pressure cascade impactor where they are classified into size of 7 nm to 10 m according to their aerodynamic diameter which determines their deposition at a particular ELPI stage. Finally, the charges carried by the aerosols are continuously measured at each impactor stage by sensitive electrometers. The measured current values are converted to give a number of particles by cm^3 using transfer functions provided by manufacturers. The transport line is an antistatic PTFE pipe heated at 180℃ to avoid effects of condensed humidity on the measurement. A vacuum pump is set to ensure an isokinetic sampling flow at a rate of 10 L/min. Double dilution of the effluents is set upstream the ELPI particle sizer with two diluters DI-1000 from Dekati. The first one is heated at 2000℃ to avoid loss in aerosol concentration while the second one prevents nucleation of the aerosols. The diluters are set in series to provide a ratio of dilution of 83.

2.4. Experimental Procedure

Samples are tested in the horizontal orientation. The sample holder is used with a frame to reduce the exposed surface of the sample. A 64 kg/m^3 ceramic fiber insulation pad is put on the backside of the sample as specified in the ISO 5660–1 standard [4]. The volumetric flow rate of extraction through the exhaust duct of

Journal : 10694_FIRE | Dispatch : 19-12-2023 | Pages : 26
MS NO : 1518 | LE ☑ CP | TYPESET ☑ DISK

the calorimeter is set at 24 ± 2 L/s at 23 ℃. The inlet volume flow rate is set at 150 ± 5 L/min at 23 ℃. Tests are carried out at 50 and 20 kW/m^2 and at 21, 18, 15 and 10 vol% of oxygen respectively. All tests are performed at least three times and the curve presented represents a single specimen that best fits the mean curve. Data were collected with a 1 s sampling interval for the cone measurement, 1 s for the ELPI and 1.76 s for the FTIR.

3. Results and Discussion

The reaction to fire of Cross-Laminated Timber is strongly dependent on the environment conditions such as the oxygen level and the heat flux. The combustion is considered incomplete when the CO/CO_2 ratio is greater than 0.05 [25]. For the whole study, the time to ignition is defined as t_i, the time to flameout as t_f, the peak of HRR as pHRR and the peak of MLR as pMLR.

3.1. Influence of Oxygen Level at 50 kW/m^2

3.1.1. Mass Loss and Heat Release 3.1.1.1. Mass Loss The influence of oxygen level on the remaining mass and the mass loss rate at 50 kW/m^2 was first studied (Figure 3. The decomposition process of CLT at 21 vol% O_2 is first described before studying the effect of oxygen.

The decomposition pathway of CLT at 21 vol% O_2 is assessed via the mass loss (Figure 3b). First, between 0 and 19 s, as the temperature at the surface of CLT increases, the sample starts to degrade. The free water contained in wood (around 11%) evaporates. Simultaneously, the chemical bonds of wood polymer chains (cellulose, hemicellulose and lignin) start to break [26, 27]. Consequently, tars and decomposition gases are produced. As the gases leave the solid, they encounter the oxygen present in the atmosphere. Concurrently, oxygen may diffuse into the solid and oxidize the wood effluents. Triggered by the igniter, the mixture ignites and the flame spreads onto the whole surface of the sample. It results, in a second step, in a fast increase of the MLR, which reaches a maximum at 60 s. A carbonaceous layer is formed on top of the wood, which reduces the heat transfers between the wood surface and the pyrolysis front. This carbonaceous layer creates then a thermal insulation [28]. As a result, pyrolysis of wood slows down and the MLR decreases. From 200 s, a small increase in MLR occurs. To understand this behavior, five thermocouples were inserted in CLT at 2, 10, 20, 30 and 38 mm from the exposed surface. When the MLR increased, the thermocouple inserted at 10 mm from the surface reached a 100 ℃ plateau (not shown). This temperature is assigned to water evolution and suggests that CLT undergoes dehydration reactions [29]. At longer times (t > 200 s), the sample reaches a thermal steady state, which is characterized by a quasi-constant MLR (Figure 3b) and a constant thickness of char layer [30]. In a next step, a second peak of MLR occurs around 2500 s. At this peak, the temperature measured at 38 mm from the surface of CLT is 320 ℃. It means that the pyrolysis front reaches the back of the sample and thus the ceramic holder induces a thermal feedback (accumulation of heat) that accelerates the decomposition [28]. Finally, flame extinguishes as the fuel con-

Journal : 10694_FIRE | Dispatch : 19-12-2023 | Pages : 26
MS NO : 1518 | LE | CP | TYPESET | DISK

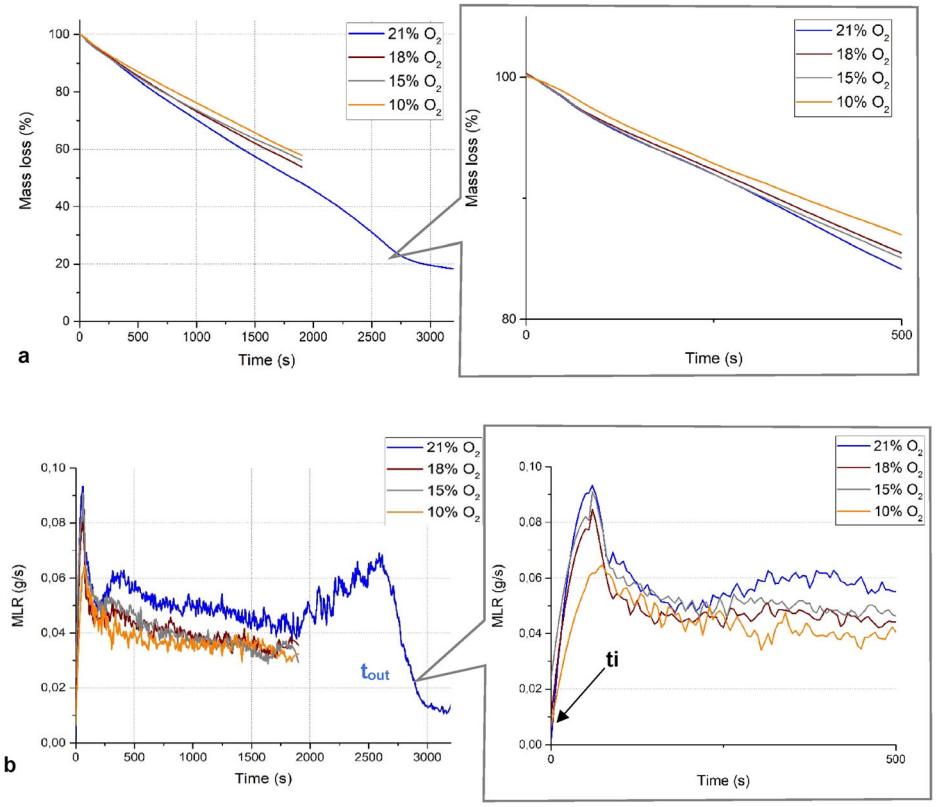

Figure 3. Effect of oxygen concentration on: (a) mass loss, (b) MLR.

tained in the solid phase diminishes and the MLR then decreases. Smoldering will then take place in the remaining char (visual observation).

Furthermore, the oxygen level affects the combustion process of CLT. Indeed, its decomposition occurs with flames at 21, 18 and 15 vol% O_2 but without flames at 10 vol% O_2. However, the MLR curves have all the same shape whatever the oxygen level (Figure 3b). The chemical reactions occurring in the condensed phase do not depend on the mass fraction of oxygen. Indeed, before 105 s, the mass loss curves and the peak of MLR (at ignition) at 21, 18 and 15 vol% O_2 (Figure 3a), (Table 2) are similar. This suggests that at the early stage of the test, the heat received at the surface of CLT mainly governs the decomposition of the sample. However, oxygen does modify the kinetics of decomposition, which are accelerated at high oxygen level. After 105 s, the mass loss of the specimen at 21 vol% O_2 accelerates while the mass losses at 18 and 15 vol% O_2 remain close with less than 0.7% of difference between them. Nevertheless, after 1100 s, the decomposition becomes faster at 18 vol% O_2 (Figure 3a). Indeed, the decrease in oxygen level reduces the flame temperature and thus the flame thermal feedback to the surface of the solid [30]. Consequently, as less heat is transferred to the pyrolysis

Journal : 10694_FIRE | Dispatch : 19-12-2023 | Pages : 26
MS NO : 1518 | ☐ LE ☑ CP | ☐ TYPESET ☑ DISK

Table 2
Influence of Oxygen on the Fire Parameters at 50 kW/m²

Oxygen level (%)	t_i (s)	pMLR (g/s)	pHRR (kW/m^2)
21	19	0.093	143
Standard error	1.5	0.004	12
18	18	0.085	138
Standard error	1.5	0.009	8
15	21	0.091	141
Standard error	0.7	0.010	9
10	–	0.065	41
Standard error		0.019	13

front with decreasing oxygen, the decomposition rate of wood is slower and the amount of CLT residue after 32 min is 48% at 21 vol% O_2 vs. 56% at 15 vol% O_2 (Figure 4) [27]. At 10 vol% O_2, the MLR curve has the same shape as other oxygen levels but the decomposition occurs without flames. Though the heat flux is high enough to decompose the sample into volatiles, there is not enough oxygen for a flaming combustion to occur. Thus, the pMLR is decreased by 43% compared to the pMLR at 21 vol% of O_2 (Table 2). As char is forming, the MLR slows down and reaches a quasi-steady state.

In the condensed phase, the oxygen concentration affects the combustion process (flaming or non-flaming) and the kinetics of decomposition. The higher the oxygen content, the faster the mass loss is.

3.1.1.2. Ignition and Heat Release In the gas phase, depicted here by the oxygen consumption based HRR, the reaction between the decomposition gases released from wood and the ambient air occurs near the surface of the sample. The mixture fuel/oxidant needs to reach the lean flammability limit to have a reaction of combustion. If there is enough energy produced by the reaction to overcome heat losses, the flame will spread on the whole surface of the sample [31]. For flaming combustion experiments (21, 18 and 15 vol% O_2), their times to ignition (Table 2) are not influenced by oxygen concentration as they are in the uncertainty range ($\pm$ 3 s). Moreover, the HRR curves of flaming samples have all the same shape (Figure 5). Indeed, the HRR increases rapidly to reach a peak and decreases after as char forms. Then, the HRR curve reaches a steady state. As the pHRRs are in the same range considering the standard errors of pHRRs at 21, 18 and 15% O_2 (Table 2), the oxygen concentration does not seem to have a significant influence. The steady state reached after the peak is related to the thickness of the char layer which is almost constant [31]. With the decrease of oxygen concentration, the layer of char becomes thicker, involving less heat transferred to the pyrolysis front. As a result, at the steady state, the higher the oxygen level is, the greater the HRR is. Furthermore, at 15 vol% O_2, the weak concentration of oxygen induces a reduction in the flame intensity and thus the HRR decreases. At the end of the test, small flames are located on the edges of the specimen.

Journal : 10694_FIRE | Dispatch : 19-12-2023 | Pages : 26
MS NO : 1518 | LE | CP | TYPESET | DISK

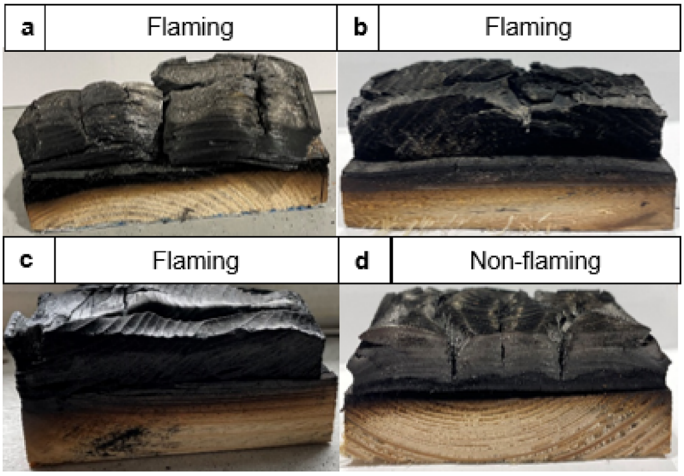

Figure 4. Sliced CLT after 32 min of test at 50 kW/m² at (a) 21% O_2, (b) 18% O_2, (c) 15% O_2 and (d) 10% O_2.

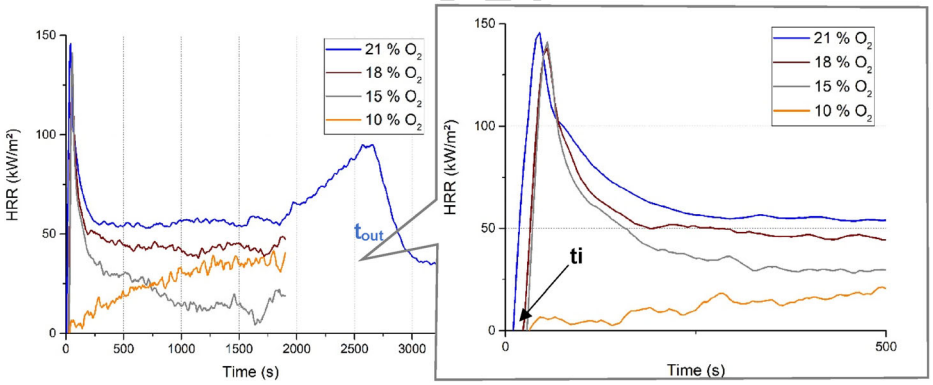

Figure 5. Effect of oxygen concentration on the HRR.

From 15 to 10 vol% O_2, the combustion switches to flaming to non-flaming mode (Figure 5). At 10 vol% O_2, the mixture fuel/oxidant remains below the flammability limit because of the lack of oxygen. Thus, the HRR is low in the early stage of the test but slowly increases next. Indeed, because of the heat received at the surface of the char, smoldering occurs. The HRR remains then steady at a level of 40 kW/m^2.

In summary, at 50 kW/m^2, two behaviors are observed according to the oxygen concentration: flaming for 21%, 18% and 15% of oxygen and non-flaming for 10% of oxygen. The pMLR and times to ignition are not affected by oxygen depletion in flaming combustion. Additionally, the oxygen concentration does not affect the pHRRs values of flaming samples but it does influence the steady state reached then.

Journal : 10694_FIRE | Dispatch : 19-12-2023 | Pages : 26
MS NO : 1518 | LE | CP | TYPESET | DISK

3.1.2. Gas Production In addition to influencing the fire parameters of the CLT, the oxygen level also has a strong influence on the gas production. The nature of gaseous products and their quantities depend on the oxygen concentration.

Wood combustion is a multi-component complex process as it is composed of three polymers: cellulose, hemicellulose and lignin. In general, thermal degradation of wood starts with the evaporation of water by dehydration reactions. Then, different chemical bonds within the polymers are broken following either depolymerization (breaking of the bonds between the monomer units of the wood polymers), fragmentation (linkage of covalent bonds of polymers) and/or char formation. This results in the release of volatile compounds and rearrangement reactions within the wood matrix. Some of the volatiles produced are unstable and may undergo secondary reactions, known as cracking (breaking of chemical bonds within the volatile compounds) or recombination (combination of volatiles compounds) [32].

More precisely, for the flaming specimens (21, 18 and 15 vol% O_2), many condensable organic compounds are identifiable on the FTIR spectra in the first events of thermal exposure. The main compounds released are formaldehyde, methanol, formic acid, acetic acid and phenol compounds. The detection of these gases is in agreement with the literature [29, 32] (Table 3), which generally ascribe their formation to fragmentation and/or breaking of chemical groups of wood polymers. Besides, the oxygen level does not alter the detection of these organic compounds nor the peak of release of formaldehyde in the early stage of the test (Figure 6c). It suggests again that the first events in wood decomposition are mainly depending on the heat level.

Then, as it blends with oxygen, this hot gaseous production oxidizes and ignition occurs. Thus, the previous mentioned organics compounds are no more detected on FTIR spectra while the production of CO_2 greatly increases. At ignition, the CO_2 emission peaks around 30000 ppm for the three oxygen levels and then reaches a steady state (Figure 6a). The high quantity of CO_2 released at ignition is due to a rapid depolymerization of wood units that gives unstable intermediaries. These intermediaries contain carboxyl and carbonyl groups that undergo fragmentation [32], for example:

$$HCOOH \rightarrow CO_2 + H_2 \text{ (decarboxylation of formic acid)}$$

$$O = CH_2 \rightarrow CO + H_2 \text{ (decarbonylation of formaldehyde).}$$

A small peak of CO, due to this depolymerization, is observed at ignition too (Figure 6b) for all flaming specimens. However, at 15 vol% O_2 and from 750 s, the CO production increases to reach a steady state and the organic species observed at ignition as well as ethene are detected. Then, from 1700s and at both 18 and 15 vol% O_2, a peak in CO emission occurs. This increase may be related to the lack of oxygen shifting the reaction of combustion towards incompleteness. Indeed, as discussed previously, flames are less intense and located on the edges of the specimen. The CO/CO_2 ratio is greater than 0.05, which means that the reac-

Journal : 10694_FIRE | Dispatch : 19-12-2023 | Pages : 26
MS NO : 1518 | LE ☑ CP | TYPESET ☑ DISK

Table 3
Organic Compounds Detected in FTIR Analysis and Their Possible Way of Formation

Organic compound	Possible way of formation [32]
Formaldehyde (CH_2O)	Fragmentation of C–C bond linked to hydroxyl groups (lignin)
Methanol (CH_3OH)	Fragmentation of methoxy groups (hemicellulose and lignin)
Formic acid (HCOOH)	Rupture of carboxylic acid functions (hemicellulose)
Acetic acid (H_3CCOOH)	Fragmentation of acetic substituents (hemicellulose)
	Reaction of C–C bonds within and between alkyl chains (lignin)
	Breaking of glycosidic linkages (cellulose)
Phenol compounds	Breaking of ether bonds between monomers units (lignin)
	Reaction of C–C bonds within and between alkyl chains (lignin)

tion of combustion is incomplete. An increase in CH_4 (Figure 6e), which is released from demethylation reactions of the remaining methyl ($–CH_3$) substituents of the residue, occurs at the same time and thus argue in favor of the combustion reaction being below stoichiometry. The more methane is produced, the more aromatic the char is [32].

For the non-flaming specimen (10 vol% O_2), in the first events of thermal exposure, the same condensable organic compounds as flaming specimens are identifiable on the FTIR spectra (Table 3). However, as the low level of oxygen slows down the kinetics of decomposition and limit oxidation, additional gases such as acetaldehyde (C_2H_4O), methane and ethene (C_2H_4) are detected [25]. As a result, a high and broad peak of formaldehyde is produced at the beginning as well as one of acetaldehyde (Figure 6c and d). Acetaldehyde can be released from the thermal decomposition of levoglucosan ($C_6H_{10}O_5$), which is an intermediate compound released from cellulose decomposition [29]. Then, a strong and broad peak of CO production follows it while the CO_2 production is very low, with a CO/CO_2 ratio of 1.37. Indeed, there is not enough oxygen to oxidize the CO produced into CO_2. Thus, the production of unburnt hydrocarbon species is also promoted, with a high production of methane throughout the experiment (Figure 6e) while a peak of ethene (23 ppm) around 120 s is detected and is followed by a peak of propene (15 ppm).

For flaming specimens (21, 18 and 15 vol% O_2), oxygen decrease favors incomplete combustion at the end of the test with an increase in CO and CH_4 production. For non-flaming conditions, smoldering promotes the production of aldehydes (formaldehyde and acetaldehyde) and unburnt gases. Thus, the production of dangerous gases is favored at low oxygen level and when the combustion is non-flaming.

Journal : 10694_FIRE | Dispatch : 19-12-2023 | Pages : 26
MS NO : 1518 | LE | CP | TYPESET | DISK

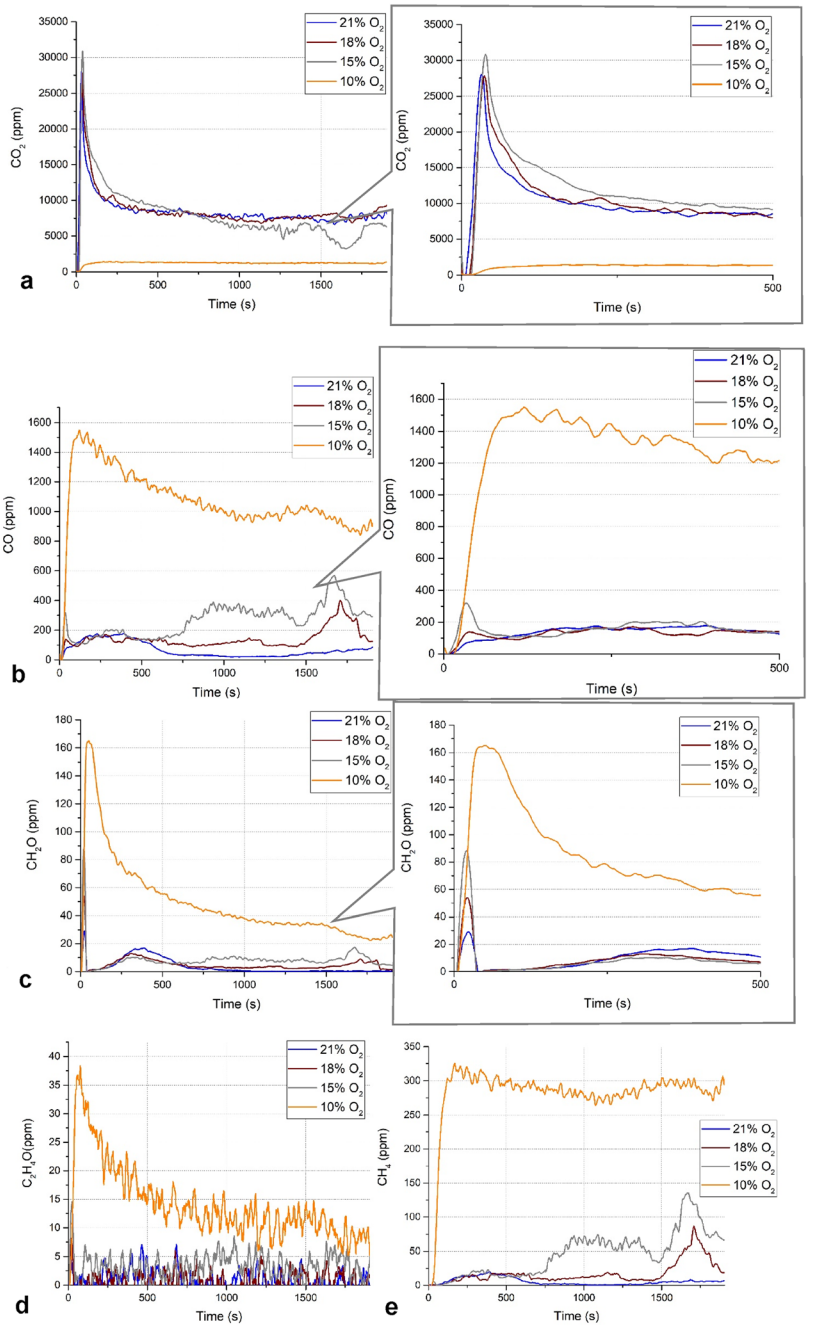

Figure 6. Influence of the oxygen level the gaseous emissions at 50 kW/m^2: (a) CO_2, (b) CO, (c) CH_2O, (d) C_2H_4O and (e) CH_4.

Journal : 10694_FIRE | Dispatch : 19-12-2023 | Pages : 26
MS NO : 1518 | ☐ LE ☑ CP | ☐ TYPESET ☑ DISK

3.2. Aerosol Production

To complete the characterization of the gas phase, the influence of oxygen on the aerosol size distribution as well as the concentration of aerosol is now investigated.

At ignition, for the three burning samples (21, 18 and 15 vol% O_2), the distribution size is bimodal and centered on the modes 0.267 m and 0.109 m (Figure 7a). This corresponds to the accumulation mode of aerosols (0.1–1 m) which indicates the agglomeration and growth of particles [33]. The concentration of aerosols in these modes is the highest at 15 vol% O_2 but the orders of magnitude are close. Then, the bimodal distribution is crushed by a great increase in the mode 0.03 m (Figure 7b). Consequently, the distribution becomes monomodal and centered on the mode 0.03 m. This now corresponds to a nucleation mode (diameter inferior to 0.1 m) representing the formation of fresh aerosols. This may be due to the nucleation of volatiles particles as the effluent mixture cools down after ignition. Indeed, vaporized gases condensed and became particles having very small size [33], [36, 37]. Globally, the concentration in this mode is of the same magnitude at 21, 18 and 15 vol% O_2.

For 10 vol% O_2, the combustion is non-flaming and the distribution is monomodal centered on the mode 0.03 m (Figure 7a). Compared to the flaming specimens, the concentration in the mode 0.03 m at 10 vol% O_2 is slightly higher (Figure 7b). In some studies, the lack of oxygen is shown to increase the number of particles. Indeed, with less oxygen available, the number of unburnt particles increases [36, 37].

For the flaming specimens, a bimodal distribution centered on the modes 0.267 m and 0.109 m is observed at ignition. Then, it is replaced by a monomodal distribution centered on the mode 0.03 m. For the non-flaming specimen, the distribution is monomodal centered on the mode 0.03 m. Globally, the distribution in size of aerosols is not influenced by oxygen level but by the combustion process.

The influence of oxygen on the reaction to fire, the gas and the aerosol production of CLT was fully assessed at 50 kW/m^2. To verify if similar behaviors are observed, it is crucial to study the influence of oxygen on less aggressive fire scenarios.

3.3. Influence of Oxygen Level at 20 kW/m^2

The reaction to fire of CLT is also strongly dependent on the thermal attack, thus the influence of the heat flux was evaluated at 20 kW/m^2. This thermal attack enables to study less aggressive fire scenarios, such as smoldering, with slower decomposition kinetics.

3.3.1. Mass Loss and Heat Release 3.3.1.1. Mass Loss The evolutions of remaining mass as a function of time (Figure 9a) are very slow and similar at the beginning of the thermal exposure whatever the oxygen concentration. However, around 550 s for 21 vol% O_2, and around 1042 s for 18 vol% O_2, the samples ignite and the mass fraction of CLT drops while the MLR reaches a peak (Fig-

Journal : 10694_FIRE | Dispatch : 19-12-2023 | Pages : 26
MS NO : 1518 | LE | CP | TYPESET | DISK

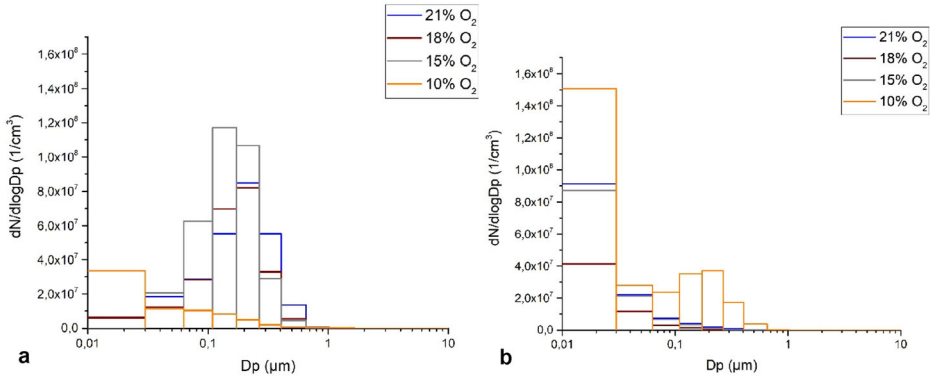

Figure 7. Distribution size of aerosols at 50 kW/m² at: (a) ti, (b) 1484 s.

ure 9b). The time to reach the peak of MLR more than doubles between 21 and 18 vol% O_2 and the pMLR is the highest for 21 vol% O_2 (Table 4). The lack of oxygen delays the ignition [38, 39] as well as the flame's temperature [40], which reduces the solid degradation rate. In the end, the samples flame out to reach a steady state around 0.25 g/s. Furthermore, the amount of CLT residue after 32 min is 68% at 21 vol% O_2 whereas it is 77% at 18 vol% O_2. The pyrolysis front has reached higher thickness at 21 vol% O_2 than at 18 vol% O_2 as the char formed is less protective (Figure 8).

At 15 and 10 of oxygen, the decomposition occurs without flames. The mass losses (Figure 9a) are similar until 700 s where the decomposition rate at 15% O_2 slightly increases. As a result, the MLRs follow a slow increase in the beginning, as water evaporates, and tend to be constant for the rest of the test (Figure 9b). The amount of CLT residue after 32 min is 81% at 15 vol% O_2 and 82% at 10 vol% O_2 (Figure 8c and d). At these low concentrations and under 20 kW/m^2, the influence of oxygen does not seem to have a significant impact on the decomposition of the CLT.

In the condensed phase, as at 50 kW/m^2, the oxygen concentration affects the combustion process (flaming or non-flaming) and the kinetics of decomposition. The higher the oxygen content is the faster the mass loss is.

3.3.1.2. Ignition and Heat Release In the gas phase, the HRR curves depict two combustion behaviors (Figure 10). Indeed, at 21% and 18% of oxygen, a peak of heat release from flaming combustion is observed while at 15% and 10% of oxygen the non-flaming decomposition is depicted by a slow and low increase in HRR. For flaming samples, the peak of HRR is reduced of 48% between the peak of HRR at 21% O_2 and the peak of HRR at 18% O_2. This is due to the low oxygen amount that does not allow a complete reaction neither a high temperature of flame. After ignition, both samples rapidly flame out. For lower oxygen levels, the HRR increases slowly to reach a steady state around 20 kW/m^2. As the behaviors are similar, the influence of oxygen seems again negligible.

Journal : 10694_FIRE | Dispatch : 19-12-2023 | Pages : 26
MS NO : 1518 | ☐ LE ☑ CP | ☐ TYPESET ☑ DISK

Table 4
Influence of Oxygen on the Fire Parameters at 20 kW/m²

Oxygen level (%)	t_i (s)	pMLR (g/s)	pHRR (kW/m^2)
21	400	0.061	96
Standard error	105	0.003	4
18	1042	0.041	51
Standard error	257	0.021	29
15	–	0.023	20
Standard error		0.034	4
10	–	0.024	22
Standard error		0.022	13

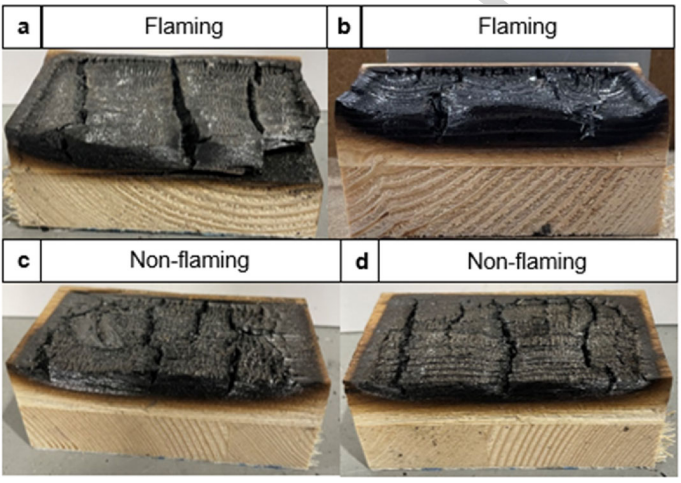

Figure 8. Sliced CLT after 32 min of test at 20 kW/m² at (a) 21% O_2, (b) 18% O_2, (c) 15% O_2 and (d) 10% O_2.

In summary, at 20 kW/m^2, two behaviors are observed according to the oxygen concentration: flaming for 21% and 18% O_2 and non-flaming for 15% and 10% O_2. The mass loss and heat release rates are similar whatever the oxygen level when the combustion is non-flaming. For flaming combustion, the ignition is delayed and less intense with oxygen decrease.

3.3.2. Gas Production For the flaming specimens (21 vol% O_2 and 18 vol% O_2), in the first events of thermal decomposition, CLT released ethene and the same organic compounds as it did at 50 kW/m^2, namely formaldehyde, methanol, formic acid, acetic acid and phenol compounds (Table 3). At 21 vol% O_2, before 200 s, a peak of formaldehyde occurs (Figure 11c). Then, at 21 vol% O_2 and from 300 s, another peak of formaldehyde is reached as well as one of CO and CH_4 (Figure 11b and d). At 400 s, the sample ignites and a peak in CO_2 occurs (Fig-

Journal : 10694_FIRE Dispatch : 19-12-2023 Pages : 26
MS NO : 1518 ☐ LE ☑ CP ☐ TYPESET ☑ DISK

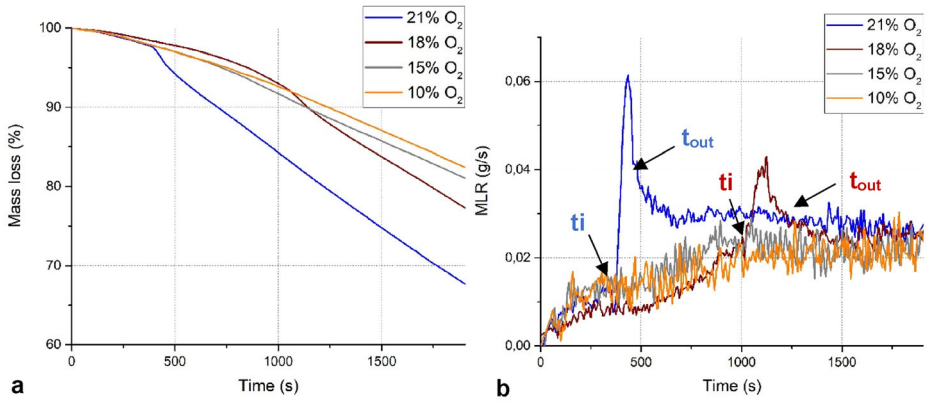

Figure 9. Effect of oxygen concentration on: (a) the mass loss, (b) the MLR.

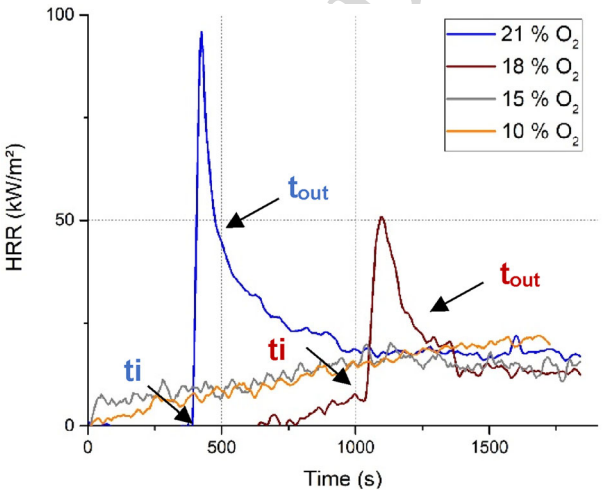

Figure 10. Effect of oxygen concentration on the HRR.

ure 11a). The CO_2 concentration rapidly decreases until the sample flames out. As a result, peaks of CH_2O, CO and CH_4 arise at 1050 s. The behavior is similar at 18 vol% O_2 but it is delayed in time. Indeed, the second peak of formaldehyde (Figure 11c) as well as these of CO and CH_4 are reached at 1035 s (Figure 11b and d). CLT ignites at 1042 s with a peak of CO_2 emission and then flames out at 1160 s with an increase in CH_2O, CO and CH_4. At the end of the test, the production of gases at 18 vol% O_2 reaches a steady state instead of decreasing as at 21 vol% O_2. In general, for both conditions, the CO/CO_2 is greater than 0.05 during the whole test (incomplete combustion). Moreover, the production of carbon dioxide is slightly higher at 21 vol% O_2 than at 18 vol% O_2 while it is the opposite for carbon monoxide and methane production.

Journal : 10694_FIRE Dispatch : 19-12-2023 Pages : 26
MS NO : 1518 LE CP TYPESET DISK

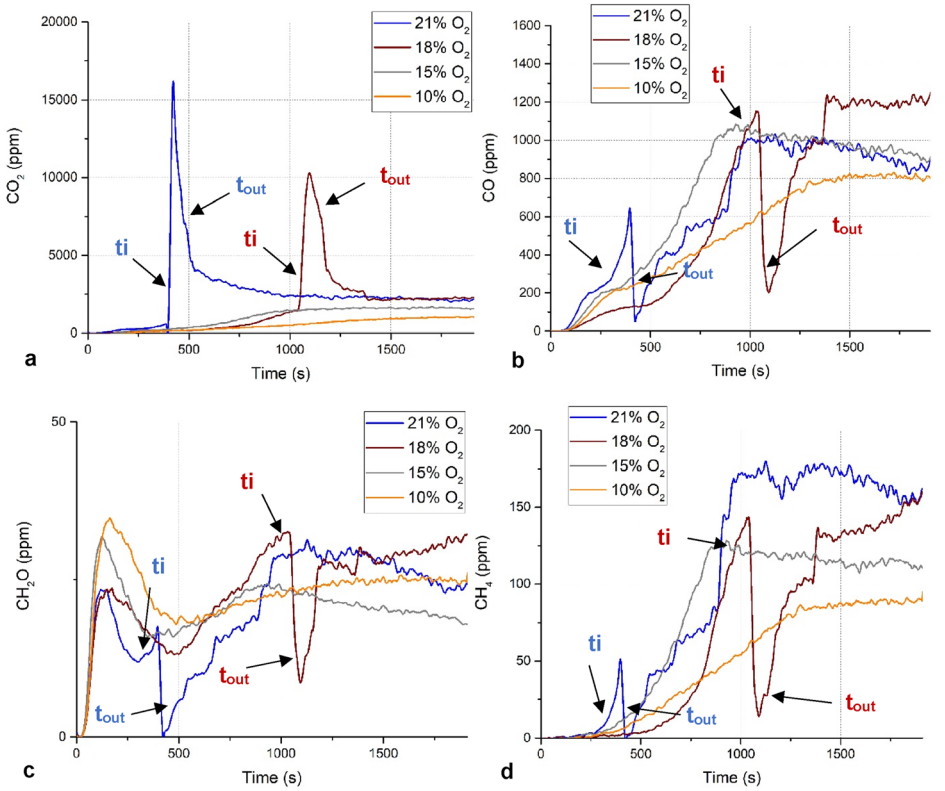

Figure 11. Influence of the oxygen level the gaseous emissions at 20 kW/m²: (a) CO_2, (b) CO, (c) CH_2O and (d) CH_4.

For non-flaming combustion (15% and 10% O_2), FTIR spectra reveal that the organic compounds produced are the same as for the flaming specimens and that they are produced during the whole test. For both oxygen levels, the CO/CO_2 ratio is greater than 0.05 during the whole test as the production of CO_2 is very low (Figure 11a). At the beginning of the test, before 250 s, a peak of formaldehyde comes up (Figure 11c) as wood decomposes and then the production drops down. In the meantime, the production in CO and CH_4 significantly increases, as wood is carbonizing, and they reach a maximum at 935 s at 15 vol% O_2 and 1500 s at 10 vol% O_2. It slightly decreases after (Figure 11a and d) and an increase in formaldehyde is also observed at these times. The same behaviors are observed at 15 vol% O_2 and 10 vol% O_2, but again the phenomena are delayed in time with oxygen decrease. For non-flaming conditions, the production of CO and CH_4 is promoted with the increase of oxygen concentration.

For flaming specimens, oxygen decrease favors incomplete combustion with higher production of CO and CH_4. However, for non-flaming conditions, the higher the oxygen level is the higher the production of CO and CH_4 is.

Journal : 10694_FIRE | Dispatch : 19-12-2023 | Pages : 26
MS NO : 1518 | LE | CP | TYPESET | DISK

3.3.3. Aerosol Production At ignition, for the burning samples at 21% O_2 and 18% O_2, the distribution is bimodal and centered on the modes 0.267 m and 0.109 m (Figure 12a), which corresponds to the accumulation mode. Then, as for 50 kW/m^2, the bimodal distribution is crushed by a great increase in the mode 0.03 m. Consequently, the distribution becomes monomodal and centered on the mode 0.03 m (Figure 12b). This corresponds again to the nucleation mode. The concentration in aerosols is slightly higher at 21% O_2 but globally of the same magnitude.

For the non-flaming specimens, the distribution is also monomodal centered on the mode 0.03 m during the whole test (Figure 12a and b). The concentration in the mode 0.03 m is similar between 15 and 10% O_2. However, it is slightly reduced compared to 21 and 18% O_2 samples. It can be due to the change in the combustion process, here smoldering which induces slower decomposition rates [34].

For the flaming specimen, a bimodal distribution centered on the modes 0.267 m and 0.109 m is observed at ignition at 21% O_2 and at 18%. Then, it is replaced by a monomodal distribution centered on 0.03 m. For the non-flaming specimen, the distribution is monomodal centered on the mode 0.03 m.

3.4. General Discussion

The fire behavior as well as the gas and aerosol production of CLT according to the oxygen concentration and the heat flux was investigated. These latter parameters are limiting factors to enable combustion as well as altering the kinetics of decomposition. The combination of both of them highlights different fire scenarios where the quantity of gases produced can be potentially toxic.

The first type of decomposition scenario obtained with CLT is flaming combustion (Figure 15). At 50 kW/m^2, the oxygen level is not high enough to disturb the combustion regime in the early stage of the test and the condensed phase is not affected. Indeed, the times to ignition (Table 2) and the maxima of MLR are similar at 21, 18 and 15 vol% O_2 (Figure 13). It could be assumed that the surface oxidation reactions would contribute to the thermal decomposition of CLT but Di Blasi [41] claims that the flame prevents the char oxidation. Oxygen cannot diffuse through the flame as it is consumed at its boundaries. Moreover, according to Kashiwagi [42], the region near the flame is poor in oxygen because of the homogenous reactions of combustion. As a result, all oxidative reactions near the surface stop. These observations are in accordance with the fact that oxygen diffusion to the surface of CLT is limited by the increased mass heat flux of gaseous products over time. As a result, the heterogeneous reactions of the solid phase cannot occur once the flame is established. However, the oxygen concentration does affect the gas phase. With oxygen decrease, the flaming combustion shifts in time to incompleteness with higher CO and CH_4 yields (Figure 14). The oxidation reactions of organic compounds into CO_2 are disadvantaged against oxidation into CO as well as demethylation at low oxygen levels. It should be noted that although the combustion regime is slightly altered with oxygen decrease, the yields in CO_2 are marginally affected. Furthermore, lowering the heat flux to 20 kW/m^2

Journal : 10694_FIRE Dispatch : 19-12-2023 Pages : 26
MS NO : 1518 ☐ LE ☑ CP ☐ TYPESET ☑ DISK

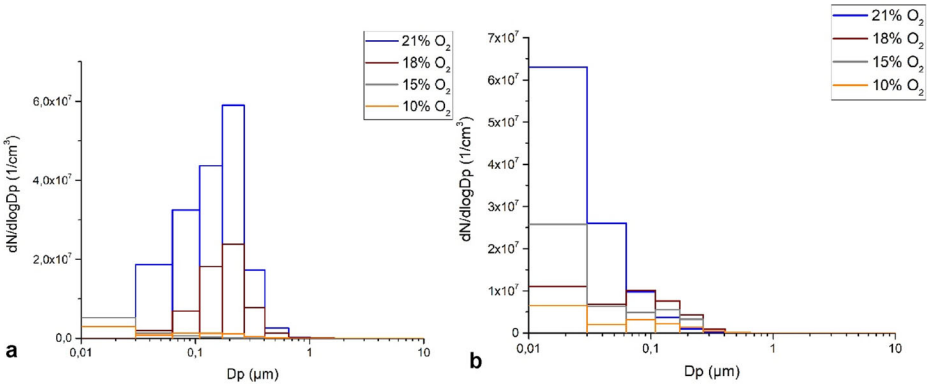

Figure 12. Distribution size of aerosols at 20 kW/m² at: (a) ti, (b) 1484 s.

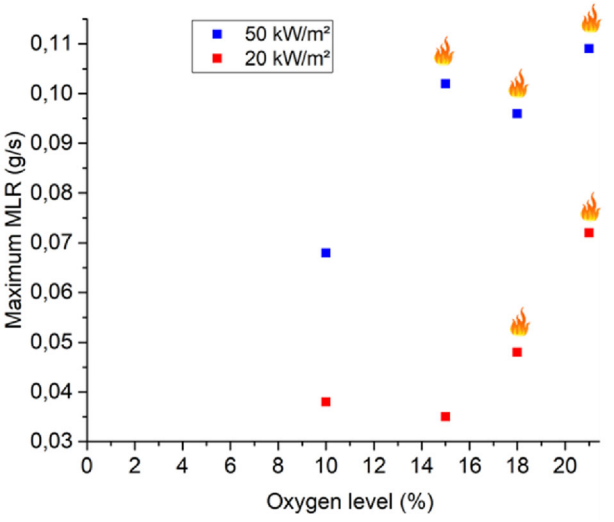

Figure 13. Effect of oxygen and heat flux on the maximum MLR.

leads to slower kinetics of decomposition (20 kW/m^2, 21 vol% O_2 and 20 kW/m^2, 18 vol% O_2). As less heat is received at the surface of CLT, the ignition process is both governed by heat and oxygen concentration. At 21 vol% O_2, the ignition of CLT is 22 times delayed in time compared to 50 kW/m^2. Similarly, at 20 kW/m^2, the time to ignition at 18 vol% O_2 is increased by a factor of 2.5 compared to the time to ignition at 18 vol% O_2. Moreover, the pMLRs are greatly lowered compared to 50 kW/m^2 (Figure 13). Between 50 and 20 kW/m^2, the pMLRs are reduced by 34% at 21 vol% O_2 and of 50% at 18 vol% O_2. Consequently, the wood matrix has time to rearrange into a more stable matrix. Indeed, before a bond can be completely broken from the wood matrix, new bonds could form to

Journal : 10694_FIRE | Dispatch : 19-12-2023 | Pages : 26
MS NO : 1518 | LE | CP | TYPESET | DISK

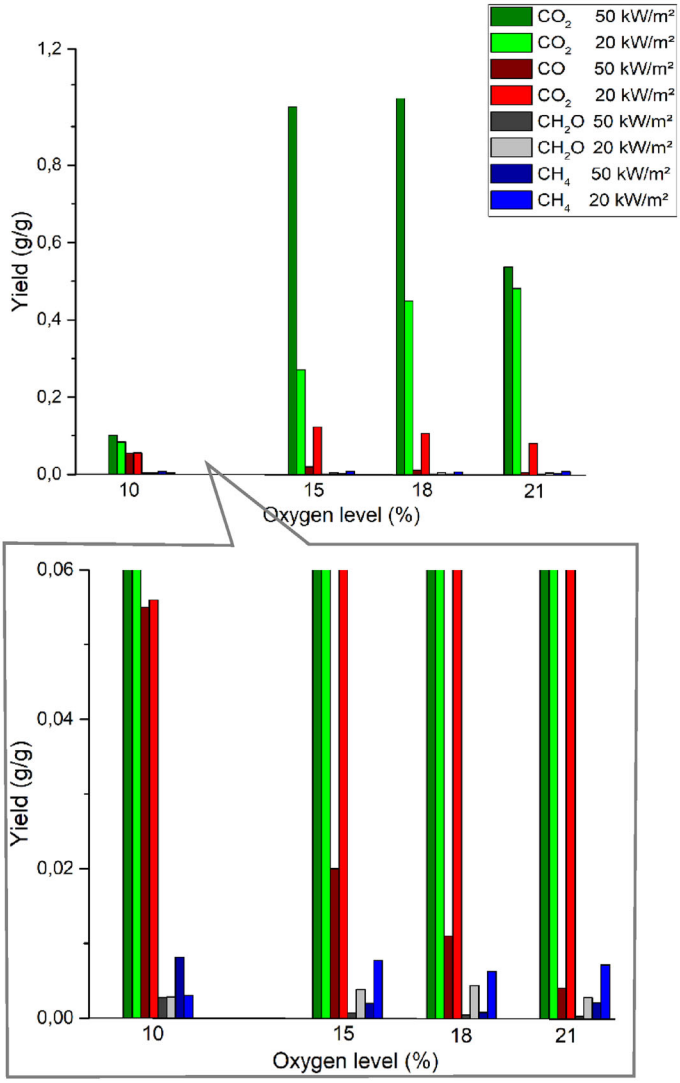

Figure 14. Total yields of CO2, CO, CH2O and CH4 as a function of oxygen level and heat flux.

bond the fragment back to the previous wood matrix [43]. Thus, less organic volatiles are produced while the yields of CO and CH_4 are promoted (Figure 14). As CLT rapidly flames out, a dramatic increase in CO and CH_4 occurs, which is amplified with oxygen decrease. For all types of flaming scenarios described, the distribution of aerosol particle size is centered on the modes 0.267 and 0.109 m at ignition and then it shifts to the mode 0.03 m. Increasing the heat flux increases the number of particles per cm^3, which is a risk as submicronic particles can penetrate the lungs [37].

Journal : 10694_FIRE | Dispatch : 19-12-2023 | Pages : 26
MS NO : 1518 | ☐ LE ☑ CP | ☐ TYPESET ☑ DISK

The second type of decomposition scenario of CLT is non-flaming combustion (Figure 15). The oxygen vitiation affects the combustion process. Indeed, at 50 kW/m^2, though the MLR curve at 10 vol% fits the shape of the flaming specimen (21, 18 and 15 vol% O_2) (Figure 3a), there is not enough oxygen to ignite the released volatiles and only smoldering occurs. However, it should be highlighted that below 21 vol% O_2 at 50 kW/m^2, the MLR curves of flaming and non-flaming specimens are close in value (around 0.4 g/s) during the steady state reached after the peak. This again suggests that the heat flux mainly governs the decomposition process and that oxygen has a low impact on it. It is also interesting to note that the pMLR reached at 10 vol% O_2 is similar to that at 21 vol% O_2 at 20 kW/m^2 (at ignition) (Figure 13). It confirms the limiting role of oxygen in the combustion regime. Moreover, the lack of oxygen increases the production of C_2H_4O (Figure 6d) and the yields of CH_4 and CO as there is not enough oxygen to oxidize organic volatiles into CO_2 (Figure 14). At high heat flux, non-flaming combustion is a threat to fire safety as the production of unburnt gases is promoted and the decomposition and heat release rates remain high. Moreover, the production of aerosols is significant which is all the more dangerous as the distribution size of aerosols is centered on the mode 0.03 m (lung penetration). Reducing the heat flux to 20 kW/m^2 leads to a higher demand in oxygen to have a flaming combustion. Indeed, the combustion is not flaming at 15 vol% O_2 whereas it was flaming at 50 kW/m^2. The low heat received at the CLT surface also results in lower decomposition rates as the pMLR is reduced by 63% between the 10 vol% O_2 cases (Figure 13). It should be underlined that the pMLR at 15 and 10 vol% O_2 are similar (Figure 13). Thus, the oxygen has no significant impact on the decomposition of the condensed phase. Moreover, the yields of CO_2 and CO are similar at 10 vol% O_2 between 50 and 20 kW/m^2 while those of CH_4 are slightly higher at 50 kW/m^2 (Figure 14). This highlights the low impact of the heat flux on gas production when the combustion is not flaming. Finally, for non-flaming combustions, the distribution of particle size is also centered on the mode 0.03 m but with a lower concentration than for flaming conditions.

4. Conclusion

The assessment of the fire behavior, the gas production and the aerosol size distribution of Cross-Laminated Timber were carried out with a homemade (based on the ISO 5660–5 standard) Controlled-Atmosphere Cone Calorimeter coupled with a FTIR and an ELPI. This is an appropriate approach to examine the effect of the oxygen and the irradiance level on the solid/gas phase phenomena occurring during the thermal degradation of CLT. Both heat flux and oxygen are revealed to be limiting factors in the combustion process, which enables the classification of fire behaviors of CLT (Figure 16).

In general, oxygen vitiation shifted the reaction of combustion towards incompleteness or even prevented it in some cases. It also greatly promoted the emission of unburnt species such as carbon monoxide and methane. These phenomena are favored at reduced heat flux. For all flaming specimens, the aerosol size distribu-

Journal : 10694_FIRE | Dispatch : 19-12-2023 | Pages : 26
MS NO : 1518 | ☐ LE ☑ CP | ☐ TYPESET ☑ DISK

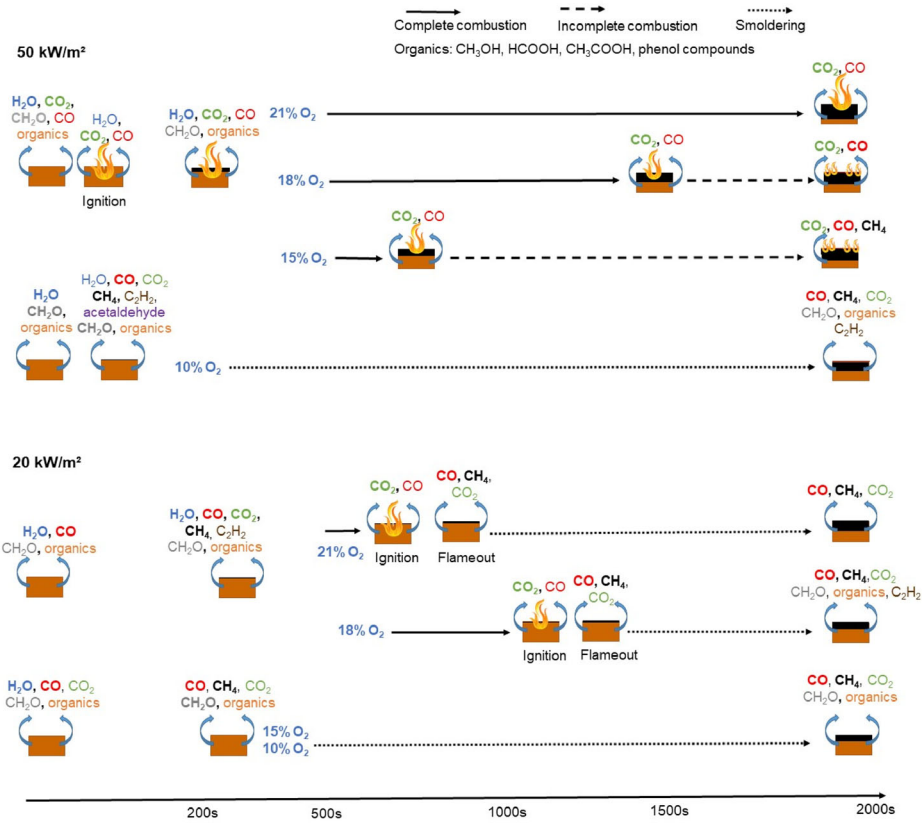

Figure 15. Flaming and non-flaming decomposition of CLT.

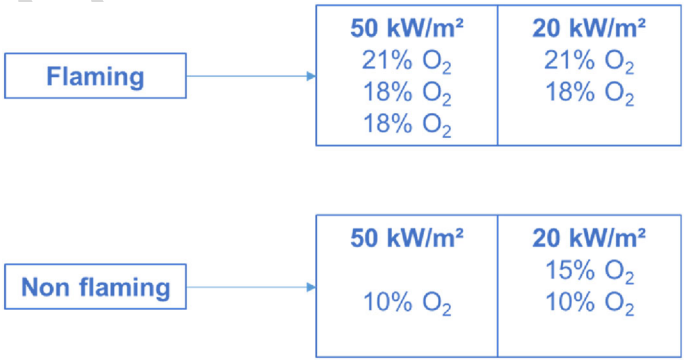

Figure 16. Classification of fire behavior of CLT according to oxygen level and heat flux.

Journal : 10694_FIRE | Dispatch : 19-12-2023 | Pages : 26
MS NO : 1518 | ☐ LE ☑ CP | ☐ TYPESET ☑ DISK

tion is centered on the modes 0.267 m and 0.109 m at ignition and then shifts to the mode 0.03 m, while for non-flaming specimens the distribution size of aerosols is centered on the mode 0.03 m.

This study highlights the hazards of different fire scenarios. CLT exposed to a high heat flux combined with low oxygen level creates an environment with a significant amount of dangerous gases and submicronic aerosols. Besides, smoldering is a hazard for fire spread in a room. Further investigations on the lower flammability limit of CLT according to oxygen level and heat flux would be interesting to have a finer understanding of its behavior. A finer measuring range of the distribution size of aerosols could be also beneficial to better assess the aerosol production.

Funding

Centre Scientifique et Technique du Bâtiment.

References

1. Hall JJ, Harwood B (1995) Smoke or burns - Which is deadlier ?. NFPA J 89(1):38–43
2. Guillaume E, Effets du feu sur les personnes, p 163
3. ISO 13571 (2012) Life-threatening components of fire—Guidelines for the estimation of time to compromised tenability in fires
4. ISO 5660–1:2015 (2015) Reaction-to-fire tests—Heat release, smoke production and mass loss rate—Part 1: heat release rate (cone calorimeter method) and smoke production rate (dynamic measurement)
5. Werrel M, Deubel JH, Krüger S, Hofmann A, Krause U (2014) The calculation of the heat release rate by oxygen consumption in a controlled-atmosphere cone calorimeter: heat release rate in a controlled-atmosphere cone calorimeter. Fire Mater 385(2):204–226. 10.1002/fam.2175
6. Marquis D, Guillaume E, Lesenechal D (2013) Accuracy (Trueness and Precision) of cone calorimeter tests with and without a vitiated air enclosure. Procedia Eng 62:103–119. 10.1016/j.proeng.2013.08.048
7. Mulholland G, Janssens M, Yusa S, Twilley W, Babrauskas V (1991) The effect of oxygen concentration on Co and smoke produced by flames. Fire Saf Sci 3:585–594. 10.3801/IAFSS.FSS.3-585
8. Nelson GL (1995) Fire and Polymers II: Materials and Tests for Hazard Prevention, in ACS Symposium Series. American Chemical Society, Washington, DC
9. Marquis D, Guillaume E, Camillo A (2014) Effects of oxygen availability on the combustion behaviour of materials in a controlled atmosphere cone calorimeter. Fire Saf Sci 11:138–151. 10.3801/IAFSS.FSS.11-138
10. Sarah C (2019) An instrumented controlled-atmosphere cone calorimeter to characterize electrical cable behavior in depleted fires, p 249
11. Etienne M, Evaluation du risque d'inflammation de gaz imbrûlés au cours d'un incendie en milieu sous-ventilé, p 283
12. Marquis DM, Guillaume E, Effects of under-ventilated conditions on the reaction-to-fire of a polyisocyanurate foam, p 13

Journal : 10694_FIRE | Dispatch : 19-12-2023 | Pages : 26
MS NO : 1518 | ☐ LE ☑ CP | ☐ TYPESET ☑ DISK

13. Hermouet F, Développement d'une approche innovante de modélisation de la cinétique de décomposition thermique des matériaux solides en espaces confinés sous-ventilés. sApplication aux incendies en tunnel, p 265
14 Swann JD, Ding Y, McKinnon MB, Stoliarov SI (2017) Controlled atmosphere pyrolysis apparatus II (CAPA II): a new tool for analysis of pyrolysis of charring and intumescent polymers. Fire Saf J 91:130–139. 10.1016/j.firesaf.2017.03.038
15. Marquis DM, Guillaume E, Camillo A, Rogaume T, Usage of controlled-atmosphere cone calorimeter to provide input data for toxicity modelling, p 13
16. Mustafa BG, Toxic species and particulate emissions from wood and pool fires, p 342
17. ISO/TS 5660–5:2020 (2020) Reaction-to-fire tests—Heat release, smoke production and mass loss rate—Part 5: heat release rate (cone calorimeter method) and smoke production rate (dynamic measurement) under reduced oxygen atmospheres
18 Tewarson A, Jiang F, Morikawa T (1993) Ventilation-controlled combustion of polymers. Combust Flame 95(1–2):151–169. 10.1016/0010-2180(93)90058-B
19 Brohez S, Marlair G, Delvosalle C (2008) The effect of oxygen concentration on CO and soot yields in fires. Fire Mater 32(3):141–158. 10.1002/fam.960
20. EN 13238:2010 (2010) Reaction to fire tests for building products - Conditioning procedures and general rules for selection of substrates
21. Alarifi A, Andrews G, Witty L, Phylaktou H (2013) Ignition and toxicity of selected aircraft interior materials using the cone calorimeter and FTIR analysis, Proceedings of the InterFlam 2013. InterScience Communications: London, UK. 1: 37–48, ISBN: 978-0-9556548-9-3
22. Irshad A, Andrews G, Phylaktou H, Gibbs B (2019) International seminar on fire and explosion hazards (9; 2019; Saint Petersburg, Russia). Develop Control Atmos Cone Calorim Simulate Compart Fires . 10.18720/SPBPU/2/K19-90
23. Ngohang FE, Combination of mass loss cone, Fourier transform infrared spectroscopy and electrical low pressure impactor to extend fire behaviour characterization of materials, p 155
24. ISO 19706:2011 (2011) Guidelines for assessing the fire threat to people
25 Stec AA, Hull R (2010) Fire Toxicity. Woodhead Publishing, Sawston
26. Friquin KL (2011) Material properties and external factors influencing the charring rate of solid wood and glue-laminated timber. Fire Mater 325(5):303–327. 10.1002/fam.1055
27 Di Blasi C, Hernandez HG, Santoro A (2000) Radiative Pyrolysis of Single Moist Wood Particles. American Chemical Society, Washington, DC
28. Quintiere JG, Rhodes B (1994) Fire growth models for materials, National Institute of Standards and Technology
29 Sullivan AL, Ball R (2012) Thermal decomposition and combustion chemistry of cellulosic biomass. Atmos Environ 47:133–141. 10.1016/j.atmosenv.2011.11.022
30 Cuevas J, Torero JL, Maluk C (2021) Flame extinction and burning behaviour of timber under varied oxygen concentrations. Fire Saf J 120:103087. 10.1016/j.firesaf.2020.103087
31. Mikkola E (1991) Charring of wood based materials. Fire Saf Sci 3:547–556. 10.3801/IAFSS.FSS.3-547
32 Collard F-X, Blin J (2014) A review on pyrolysis of biomass constituents: mechanisms and composition of the products obtained from the conversion of cellulose, hemicelluloses and lignin. Renew Sustain Energy Rev 38:594–608. 10.1016/j.rser.2014.06.013
33 Laaongnaun S, Patumsawad S (2022) Particulate matter characterization of the combustion emissions from agricultural waste products. Heliyon 8(8):e10392. 10.1016/j.heliyon.2022.e10392
34. Hosseini S et al (2010) Particle size distributions from laboratory-scale biomass fires using fast response instruments. Atmos Chem Phys 10(16):8065–8076

Journal : 10694_FIRE | Dispatch : 19-12-2023 | Pages : 26
MS NO : 1518 | LE ☑ CP | TYPESET ☑ DISK

35 Lighty JS, Veranth JM, Sarofim AF (2000) Combustion aerosols: factors governing their size and composition and implications to human health. J Air Waste Manag Assoc 50 (9):1565–1618. 10.1080/10473289.2000.10464197
36 Hertzberg T, Blomqvist P (2003) Particles from fires: a screening of common materials found in buildings. Fire Mater 27(6):295–314. 10.1002/fam.837
37. Nussbaumer T, Czasch C, Klippel N, Johansson L, Tullin C 9, Particulate Emissions from Biomass Combustion in IEA Countries. p 40
38 Hurley MJ et al (2016) SFPE Handbook of Fire Protection Engineering. Springer, New York. 10.1007/978-1-4939-2565-0
39 Delichatsios MA (2005) Piloted ignition times, critical heat fluxes and mass loss rates at reduced oxygen atmospheres. Fire Saf J 40(3):197–212. 10.1016/j.firesaf.2004.11.005
40 Ohlemiller TJ, Kashiwagi T, Werner K (1987) Wood gasification at fire level heat fluxes. Combust Flame 69(2):155–170. 10.1016/0010-2180(87)90028-9
41. Di Blasi C (2004) The burning of plastics. In: Troitzsch J (ed) Plastics Flammability Handbook, Principles Regulation Testing and Approval Carl Hanser Verlag GmbH & Co KG, München, pp 47–132
42 Kashiwagi T (1994) Polymer combustion and flammability—Role of the condensed phase. Symp (Int) Combust 25(1):1423–1437. 10.1016/S0082-0784(06)80786-1
43 Shen J, Wang X-S, Garcia-Perez M, Mourant D, Rhodes MJ, Li C-Z (2009) Effects of particle size on the fast pyrolysis of oil mallee woody biomass. Fuel 88(10):1810–1817. 10.1016/j.fuel.2009.05.001